Interaction, growth, and ordering of epitaxial graphene on SiC{0001} surfaces: A comparative photoelectron spectroscopy study

K. V. Emtsev, F. Speck, Th. Seyller,* and L. Ley
Lehrstuhl für Technische Physik, Universität Erlangen-Nürnberg, Erwin-Rommel-Strasse 1, 91058 Erlangen, Germany

J. D. Riley
Department of Physics, La Trobe University, Bundoora, Victoria 3083, Australia
(Received 11 July 2007; revised manuscript received 3 March 2008; published 2 April 2008)

Thermally induced growth of graphene on the two polar surfaces of 6*H*-SiC is investigated with emphasis on the initial stages of growth and interface structure. The experimental methods employed are angle-resolved valence band photoelectron spectroscopy, soft x-ray induced core-level spectroscopy, and low-energy electron diffraction. On the Si-terminated (0001) surface, the $(6\sqrt{3}\times 6\sqrt{3})R30°$ reconstruction is the precursor of the growth of graphene and it persists at the interface upon the growth of few layer graphene (FLG). The $(6\sqrt{3}\times 6\sqrt{3})R30°$ structure is a carbon layer with graphene-like atomic arrangement covalently bonded to the substrate where it is responsible for the azimuthal ordering of FLG on SiC(0001). In contrast, the interaction between graphene and the C-terminated $(000\bar{1})$ surface is much weaker, which accounts for the low degree of order of FLG on this surface. A model for the growth of FLG on SiC{0001} is developed, wherein each new graphene layer is formed at the bottom of the existing stack rather than on its top. This model yields, in conjunction with the differences in the interfacial bonding strength, a natural explanation for the different degrees of azimuthal order observed for FLG on the two surfaces.

DOI: 10.1103/PhysRevB.77.155303 PACS number(s): 73.20.At, 68.35.B−, 68.35.Ct, 79.60.−i

I. INTRODUCTION

Graphene, a single sheet of sp^2-bonded carbon arranged in a honeycomb lattice, has unusual electronic properties that arise from the linear dispersion of the π and π^* bands in the vicinity of the K point of the hexagonal Brillouin zone.[1–7] The crossing of these bands (the Dirac point E_D) marks the Fermi energy in neutral graphene. Graphene's most important properties from a technological point of view are the ambipolar field effect, the high carrier mobility, currently of the order of a few $m^2\ V^{-1}\ s^{-1}$, and the low contact resistance to metals.[8] Thus, graphene represents the ideal two-dimensional electron gas system and it raises high hopes that it will find its way into new high-speed, ballistic-transport-based electronic devices.[5,8]

Many exciting results were produced by using exfoliated graphene,[2–4,6,7] but it can be debated whether this preparation is suitable for technological processes where large areas of uniform graphene are required. Solid state graphitization of silicon carbide (SiC) surfaces[9–16] by annealing of SiC at temperatures above 1150 °C has the potential to fulfill the requirement for a large scale production of graphene-based devices.[1,5]

The growth of ultrathin graphite layers, so-called few layer graphene (FLG), has been carried out on the Si-terminated (0001) and C-terminated $(000\bar{1})$ surfaces with somewhat different results.[1,5,9–16] On SiC(0001), where a $(6\sqrt{3}\times 6\sqrt{3})R30°$ reconstruction ($6\sqrt{3}$ for short) is observed at the very beginning of growth, the FLG layers are aligned with respect to the substrate so that the primitive translation vectors of FLG and SiC enclose an angle of 30°. The FLG layers on SiC$(000\bar{1})$ consist of rotationally disordered domains as witnessed by diffraction rings observed in low-energy electron diffraction (LEED). However, the rings frequently show an intensity modulation, indicating a certain preference for alignment with respect to the substrate. Furthermore, there is also experimental evidence that the individual graphene layers in thicker FLG films on SiC$(000\bar{1})$ contain rotational stacking faults.[17,18] Both the misalignment with respect to the substrate and the turbostratic structure of the films were recently explained in terms of higher order commensurate structures of the growing graphene layers, which leads to preferred but rotated orientations of the first graphene layer on the SiC$(000\bar{1})$ substrate and also of the individual graphene layers with respect to each other.[17]

Recently, two theoretical studies investigated the electronic structure of the interface between polar SiC{0001} surfaces and FLG.[19–21] For computational reasons, both groups considered a hypothetical $(\sqrt{3}\times\sqrt{3})R30°$ surface unit mesh with a covalently bound graphene layer that requires a dilation of the C-C distance by 8% in order to accommodate the smaller unit cell. We will refer to this model as the "covalently bound stretched graphene" (CSG) model. A top view of this model is shown in Fig. 1. Note that the model requires one unsaturated Si atom in the $(\sqrt{3}\times\sqrt{3})R30°$ unit mesh. Both studies found that the first carbon layer does not exhibit graphene-like electronic properties. The latter are obtained by the second layer only, which is bound by weak dispersion forces to the first layer.

In the absence of calculations for the correct structure, an experimental study of the electronic structure such as presented here is extremely important. By connecting the experimental results to the above mentioned calculations, we can clearly distinguish between aspects which stem from the wrong choice of unit cell and those that do not. In this way we answer the following important questions. (a) Is the hypothetical model a valid approximation? (b) Which conclusions can be drawn from calculations for the hypothetical

 ©2008 The American Physical Society

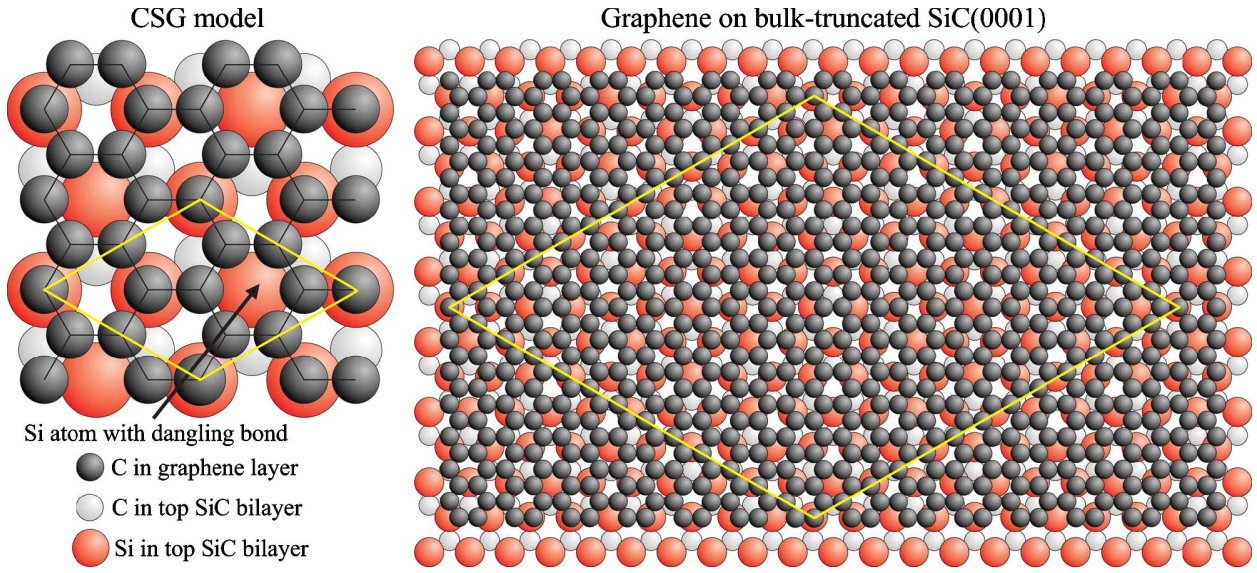

FIG. 1. (Color online) Left: Top view of the CSG model on SiC(0001). The large diamond shows the $(\sqrt{3}\times\sqrt{3})R30°$ unit mesh of the model surface. Note that the structure has one dangling bond per unit mesh due to an unsaturated Si atom. For the CSG model on SiC(000$\bar{1}$), the roles of the substrate C and Si atoms are interchanged. Right: A monolayer graphene placed on the bulk-truncated SiC(0001) surface. The large diamond indicates the unit cell of the resulting $6\sqrt{3}$ coincidence lattice, which contains 169 graphene unit cells and 108 SiC(0001) unit meshes.

model? (c) Which cannot? Therefore, in this work we study the electronic structure of the interface between SiC and graphene by using angle-resolved photoelectron spectroscopy (ARPES), high-resolution core-level soft x-ray photoelectron spectroscopy (SXPS) employing synchrotron radiation, and LEED. Our results show that the interaction of FLG with the underlying surface is quite different for the two surface polarities. For the Si-terminated SiC(0001) surface, a strong interaction of the first layer with the substrate is observed, while on the C face, we see weak interaction. This observation explains the structural differences of the FLG films. Hence, the CSG model is—within limitations to be described below—a reasonable approximation for the $6\sqrt{3}$ structure on SiC(0001), but it fails to correctly describe the interface between SiC(000$\bar{1}$) and FLG.

II. EXPERIMENT

FLG growth was carried out *in situ* in ultrahigh vacuum on *n*-type $[(1-2)\times10^{18}\ \mathrm{cm}^{-3}]$ 6*H*-SiC{0001} as described elsewhere.[22] In order to remove surface oxides, samples were first exposed to a Si flux at 950 °C; Si was gradually removed from the surface by annealing steps at increasing temperatures between 1150 and 1400 °C until FLG growth commenced. The sequence of surface reconstructions observed during the preparation is face dependent.[23] On SiC(0001), the sequence is (3×3), $(\sqrt{3}\times\sqrt{3})R30°$, $6\sqrt{3}$, and $(1\times1)_{\mathrm{graph}}$. On SiC(000$\bar{1}$), different reconstructions occur: $(2\times2)_{\mathrm{Si}}$, (3×3), $(2\times2)_{\mathrm{C}}$, and $(1\times1)_{\mathrm{graph}}$, with the $(2\times2)_{\mathrm{C}}$ showing up just in a small temperature region and in coexistence with the (3×3) and $(1\times1)_{\mathrm{graph}}$ structures, respectively.

ARPES measurements were carried out at room temperature by using a toroidal electron analyzer with a total energy and an angle resolution of 120 mV and 0.2, respectively.[24] High-resolution core-level spectra were acquired by using a hemispherical analyzer (Specs, Phoibos150) with a total energy resolution of 75/120 meV at $\hbar\omega$==350/510 eV. All measurements were performed at the storage ring BESSY II. All energies of electronic structures throughout the paper are binding energies referenced to the Fermi energy (E_F).

III. RESULTS

A. SiC(0001)

In Fig. 2, we show the valence band dispersion measured along the $\bar{\Gamma}\bar{K}$ and $\bar{\Gamma}\bar{M}$ azimuths in the graphene Brillouin zone (BZ) as well as the LEED patterns obtained after annealing of the 6*H*-SiC(0001) surface at 1150 and 1250 °C, respectively. These temperatures correspond to two consecutive stages of graphitization, namely, the C-rich $6\sqrt{3}$ reconstruction and the first graphene layer, respectively. The LEED patterns taken on the two surfaces [Figs. 2(c) and 2(d)] differ only slightly in that the LEED spots corresponding to the graphene reciprocal lattice become somewhat stronger upon the formation of the first graphene layer. In agreement with previous results, we observe that the graphene layers are aligned with the substrate.[1,5,9–11,14–16,22]

On the other hand, the electronic structures of the $6\sqrt{3}$ reconstruction and the first graphene layer differ significantly in some aspects, whereas they are surprisingly similar in others [Figs. 2(a) and 2(b)]. First of all, the valence band structure of the $6\sqrt{3}$ reconstruction shown in Fig. 2(a) exhibits graphene-like σ bands between 5.1 and 22.7 eV binding en-

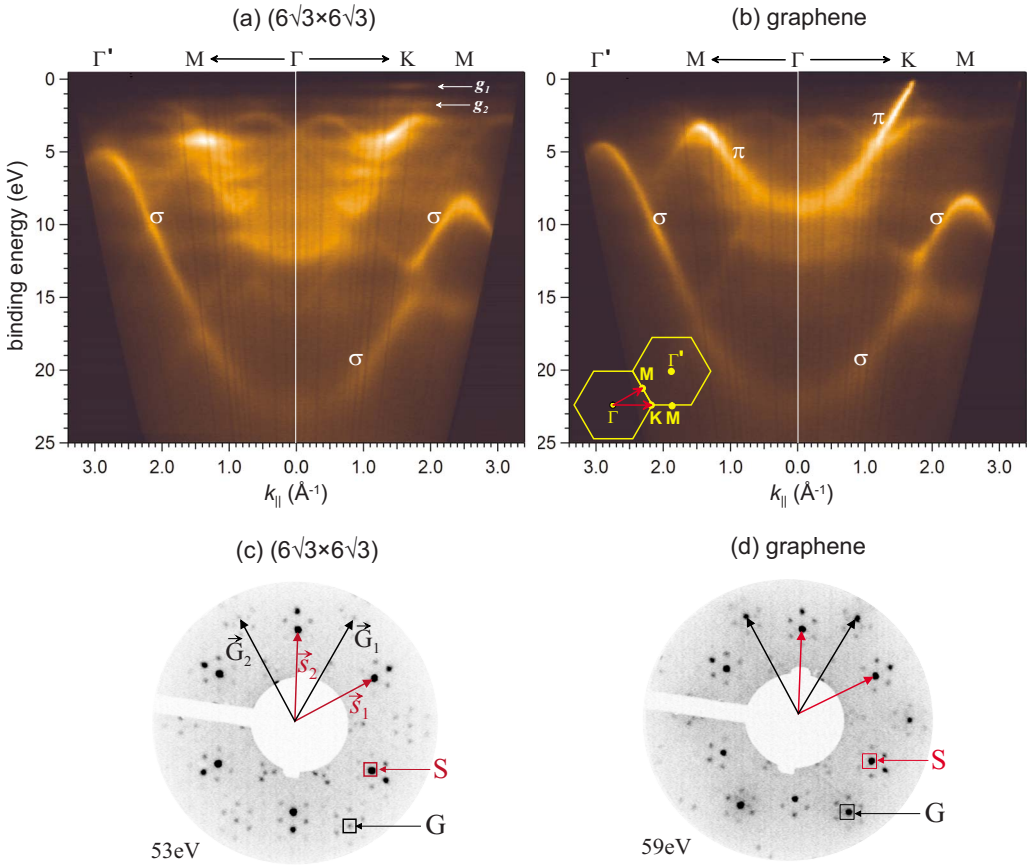

FIG. 2. (Color online) Photoelectron intensity map vs binding energy and parallel electron momentum of (a) SiC(0001)$-6\sqrt{3}$ and (b) 1 ML graphene on top of SiC(0001)$-6\sqrt{3}$ ($h\nu$=50 eV). The inset shows the direction of $k_{\|}$ within the hexagonal Brillouin zone of graphene. LEED patterns of the (c) $6\sqrt{3}$ reconstruction and (d) 1 ML graphene on 6H-SiC(0001). The reciprocal lattice vectors of the SiC ($\vec{s}_1,\vec{s}_2$) and graphene ($\vec{G}_1,\vec{G}_2$) lattices are indicated. Linear combinations of either $\vec{s}_1$ and $\vec{s}_2$ only or $\vec{G}_1$ and $\vec{G}_2$ only lead to the first order diffraction spots S and G of SiC and graphene, respectively. Examples are indicated. The remaining spots can be constructed by linear combinations of $\vec{s}_1$, $\vec{s}_2$, $\vec{G}_1$, and $\vec{G}_2$. These are the diffraction spots characteristic of the $6\sqrt{3}$ reconstruction.

ergies, which are well developed in both energetic band width and periodicity in momentum space as judged from a comparison with the σ bands of the first graphene layer shown in Fig. 2(b). This implies that the atomic arrangement within the $6\sqrt{3}$-reconstructed layer is topologically identical to that of graphene, i.e., that it contains six-membered rings only and no five- or seven-membered rings.[25] The fact that the width of the sigma band (17.6 eV) is the same for the $6\sqrt{3}$ reconstruction and for graphene indicates that the average C-C bond length must be identical. This is further supported by the observation that the extensions of the Brillouin zones of graphene and the $6\sqrt{3}$ reconstruction are in excellent agreement. The σ bands of the $6\sqrt{3}$ reconstruction layer are shifted by 1.0 ± 0.1 eV toward higher binding energies with respect to those of neutral graphite. This is also demonstrated in Fig. 3(c), which shows energy distribution curves (EDCs) for the $6\sqrt{3}$ reconstruction, monolayer graphene, bilayer graphene, and graphite for $k_{\|}$ corresponding to Γ' as defined in Fig. 2. For monolayer graphene [Figs. 2(b) and 3(c)], this shift is reduced to 0.4 eV with respect to graphite. The same shift was reported for the Dirac point E_D of the first graphene layer relative to E_F in previous studies.[26–28] It is attributed to a partial filling of the π^* bands due to charge transfer from the substrate.

At the same time, the $6\sqrt{3}$ reconstruction fails to exhibit graphene-like π bands altogether although there is an accumulation of intensity centered around Γ with an envelope that is suggestive of the dispersion of the π band. We attribute this to band folding[29] caused by the potential of the large unit cell, which affects the delocalized π states stronger than the more localized σ states. The individual bands that are not fully resolved due to the large unit cell of the $6\sqrt{3}$ reconstruction show a spectral weight that follows the original unfolded band.[29] The bottom of this band at Γ lies 3.2 eV lower than the bottom of the π band of graphene, which indicates a considerable covalent coupling of p_z orbitals to the substrate. A similar effect, that is, a significant lowering of the π band, was observed earlier for a monolayer of graphite on a Ni(111) surface and was attributed to a hybridization of the π states with the states of the substrate.[30] In the Ni case, however, no band folding is observed since the graphene layer is commensurate with the Ni(111) surface.

The $6\sqrt{3}$ reconstruction is nonmetallic, i.e., there are no states at the Fermi level. Only two localized states (g_1 and g_2) exist in the region close to E_F [Fig. 2(a)]. Their binding

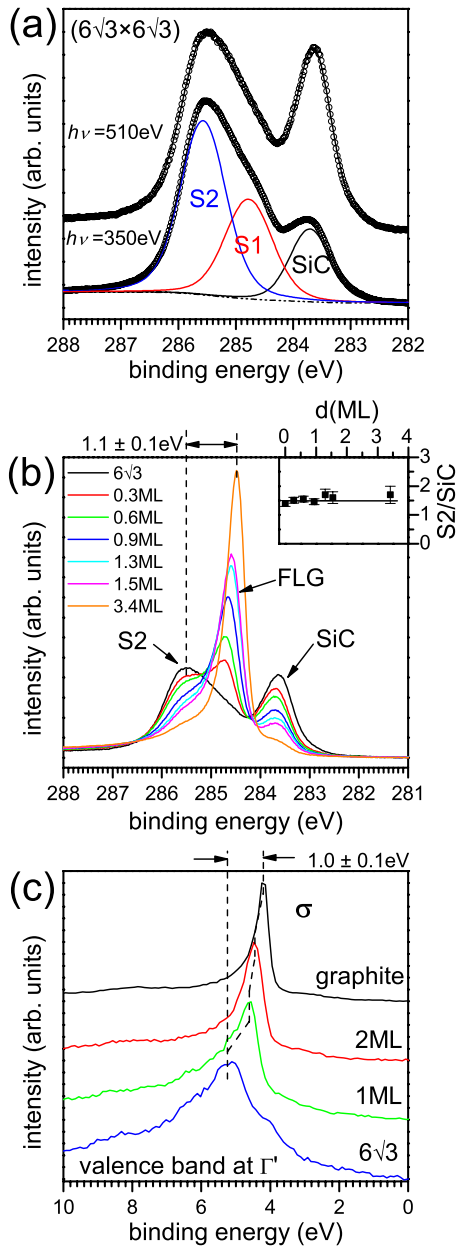

FIG. 3. (Color online) (a) C 1*s* core-level spectra of the SiC(0001)$-6\sqrt{3}$ reconstruction. (b) Evolution of the C 1*s* core-level spectrum upon growth of up to 3.4 layers of graphene (FLG). The inset shows the intensity ratio of component S2 to bulk component SiC for measurements at $h\nu$=510 eV as a function of FLG thickness. d=0 corresponds to the $6\sqrt{3}$ reconstruction. (c) EDCs taken at Γ (see Fig. 2) of the $6\sqrt{3}$ reconstruction, graphene, bilayer graphene, and graphite. The peak corresponds to the maximum of the σ band. Note the energy difference of (1.0 ± 0.1) eV between the σ-band maximum of the $6\sqrt{3}$ reconstruction and graphite.

energies are 0.5 and 1.6 eV, respectively. Hence, the electronic structure of the $6\sqrt{3}$ reconstruction is obviously quite different from that of graphene, where delocalized π states extend right to the Fermi level, as can be seen in Fig. 2(b). The nonmetallic character of the $6\sqrt{3}$ surface is another result that supports the notion of a strong interaction of, at least, part of the carbon p_z orbitals with the substrate. Indeed, recent theoretical studies demonstrate that covalent bonding of, for example, hydrogen to graphene considerably changes the electronic structure of the π bands. Two extreme cases of hydrogen covalently bonded to graphene have been considered: graphane, where all C atoms are bonded to hydrogen,[31] and a situation where one H atom is bonded per (4×4) supercell.[32] In either case, a gap (3.5 and 1.25 eV, respectively) opens in the graphene band structure due to the covalent bonds and the accompanying rehybridization.

The strong coupling of parts of the C atoms in the reconstruction layer to the substrate is further illuminated by the high-resolution C 1*s* spectra shown in Figs. 3(a) and 3(b) for various stages of FLG growth. Note that raw data are shown and that the noise level present in the data is much lower than in previously published studies.[10,33] The spectra of the $6\sqrt{3}$ reconstruction in Fig. 3(a) consist of a SiC bulk component at 283.70 ± 0.08 eV and two surface components S1 and S2 at 284.75 ± 0.10 and 285.55 ± 0.10 eV, respectively. The intensity ratio $S1:S2\approx0.5\pm0.05$ remains essentially constant independent of the inelastic mean free path of the photoelectrons, which was varied from 2.9 to 4.5 Å by changing the photon energy from 350 to 510 eV [see Fig. 3(a)]. This proves that the C atoms responsible for S1 and S2 are located in the same plane.

In order to estimate the thickness of the carbon layer that gives rise to S1 and S2, we used the conventional layer attenuation model for core-level intensities. As discussed above, we assume that the C-C bond length and, thus, the area density of C atoms are identical to those in graphene. For the $6\sqrt{3}$ reconstruction, we then obtain an effective layer thickness of 2.4 ± 0.3 Å, which is consistent with a monolayer coverage. The area density of C atoms in graphene $(3.82\times10^{15}\ \mathrm{cm}^{-2})$ is close to three times that of Si atoms on the SiC(0001) surface $(1.22\times10^{15}\ \mathrm{cm}^{-2})$. With these numbers, the S1:S2 ratio naturally follows if one-third of the C atoms in the C layer strongly interacts with the dangling bonds of the underlying SiC(0001) surface, leading to component S1. The remaining two-thirds bound to C atoms within the layer only give rise to component S2 with the higher binding energy.

Both surface components (S1 and S2) related to the $6\sqrt{3}$ reconstruction have binding energies higher than that of neutral graphite (284.42 eV). This fact agrees with a down shift of the valence σ states of the $6\sqrt{3}$ reconstruction layer with respect to bulk graphite by 1.0 eV alluded to above [see also Fig. 3(c)]. By taking into account, the magnitude of the σ-state shift as a measure of the shift in E_F we expect the C 1*s* binding energy of the respective sp^2-bonded carbon atoms to be higher than that of graphite by the same amount. That places them at ≈285.4eV, a value that coincides rather well with the position of the stronger surface component S2 $(285.55\pm0.10$ eV) and confirms our assignment of S2 to sp^2-bonded C atoms in the reconstruction layer. The other component S1 has a binding energy that lies between those of S2 and SiC. This is expected for the carbon atoms in the reconstruction layer, which are bound to one Si atom of the Si-terminated SiC(0001) surface and to three C atoms in the layer. The large widths of the components S1 and S2 (ω_G =0.9 and 0.85 eV, respectively) are a consequence of strain in the carbon layer that causes strong inhomogeneous broad-

ening. In contrast to graphite, S1 and S2 lack asymmetry due to the nonmetallic nature of the surface, which was discussed above.

Hence, the band structure measurements as well as the core-level data taken for the $6\sqrt{3}$-reconstructed surface suggest a structural model in which a graphene-like layer is bound covalently to the SiC(0001) surface by every third C atom forming a C-Si bond with the substrate. Insofar our measurements agree with the basic tenets of the CSG model; there are, however, points of disagreement, as will be discussed further in Sec. IV.

Figure 3(b) displays C 1*s* spectra obtained after further annealing steps, which led to the growth of additional graphene layers (FLG).[26–28,34] They give rise to a growing C 1*s* signal, which shifts from 284.74 ± 0.05 to 285.47 ± 0.05 eV for the largest thickness of 3.4 monolayers (ML) considered here. The shift is due to the transfer of negative charge from the substrate to the FLG film with the *proviso* that most of the charge resides close to the interface.[27,28,34] Therefore, with increasing number of layers, we probe more neutral graphene layers at the surface and the C 1*s* binding energy approaches that of graphite. Another important observation is that the component S2 of the $6\sqrt{3}$ structure is attenuated in the same way as the SiC bulk signal since the ratio of S2/SiC remains constant during graphitization [see inset of Fig. 3(b)]. This indicates that the concentration of atoms responsible for the component S2 also remains constant even for a film thickness over 3 ML. In other words, despite the fact that the progressive graphitization consumes more and more of the SiC substrate, the structure of the interface between the SiC(0001) surface and FLG is identical to that of the $6\sqrt{3}$-reconstructed layer formed during the initial stage of graphitization. Note that scanning tunneling microscopy (STM) has shown that few layer graphene films grown on SiC(0001) retain a height modulation that corresponds to the apparent (6×6) periodicity usually seen for the $6\sqrt{3}$ reconstruction.[35–39] However, the presence of the C1*s* components S2 and S1 in the C 1*s* core-level spectra reported here is a definitive proof that the same structural elements as in the $6\sqrt{3}$ reconstruction are present at the interface between FLG and SiC(0001).

B. SiC(000$\bar{1}$)

We now turn to the C face. Selected ARPES valence band spectra taken during graphitization of SiC(000$\bar{1}$) starting from the clean SiC (3×3) reconstructed surface and ending with two graphene monolayers are shown in Figs. 4(a)–4(d). The graphene coverage was determined from the C 1*s* core-level intensities taken simultaneously with ARPES datasets. Interestingly, already at a coverage of 0.3 ML, we observe the spectral signature of σ and π bands of graphene. Again, charge transfer results in a rigid shift of all bands by approximately 0.2 eV toward higher binding energy as compared to graphite. The transitions associated with SiC bulk bands are gradually attenuated until they almost completely disappear for a coverage close to a monolayer [Fig. 4(c)]. At the same time, the band structure of graphene is fully developed with regard to both σ and π bands. No perturbations of the overlayer electronic structure similar to that seen on the Si face and related to the interfacial $6\sqrt{3}$-reconstructed layer are detected for the C face. Hence, the ARPES data suggest only a weak coupling of the FLG film with the SiC(000$\bar{1}$) surface. At all coverages, we also observe the signature of rotated domains, which gives rise to an additional σ-band emission labeled σ'. Similar observations were made also for the π band. This indicates that, starting from the very beginning of growth, graphene exists in rotated domains on the SiC(000$\bar{1}$) surface.

Figures 4(e)–4(h) depict a selection of LEED images of various stages of FLG growth on 6*H*-SiC(000$\bar{1}$). The reciprocal lattice vectors of the SiC substrate $(\vec{s}_1,\vec{s}_2)$ and the graphene lattice $(\vec{G}_1,\vec{G}_2)$ are indicated. For all graphene or FLG coverages studied, the diffraction spots due to the graphene/FLG layer are smeared out into a strongly modulated diffraction ring, which indicates the presence of rotational disorder. This observation is in good agreement with previous reports.[13,16] At low coverage, the LEED images show a coexistence of the (3×3), $(2\times2)_C$, and graphitic structure as demonstrated, for example, in Fig. 4(f). At a coverage of 1 ML, the LEED pattern only contains diffraction spots from the SiC substrate with reduced intensity and from the rotationally disordered graphene layer. Other superlattice spots have vanished. This observation is in contrast to previous work. Forbeaux *et al.*[13] concluded that the initial growth of graphite on SiC(000$\bar{1}$) occurs on the (2×2) reconstruction. LEED, however, is not a local probe and averages over a large area of the surface that could contain patches of different reconstructions. In agreement with that, Hass *et al.*[17] reported a long range order of the (2×2) reconstruction of 200 Å, which is at least ten times smaller than the coherence length of the graphene film, and suggested that different parts of their surface are in different stages of graphitization. Finally, at layer thicknesses in excess of approximately 3–4 ML, the substrate spots are attenuated below the detection limit and only the smeared-out diffraction spots of the turbostratic[17,18] FLG layer prevail.

The absence of a strong coupling between the graphite overlayer and the SiC(000$\bar{1}$) substrate is further supported by the C1*s* core-level data taken at various stages of FLG growth with coverages between 0.15 and 4.3 ML, as shown in Fig. 5. By comparing the spectra to those of the Si face, it is evident that no interface related components similar to S1 and S2 are present. Instead, the spectra are dominated by two components, one of which is attributed to the SiC bulk. Its binding energy (282.5 ± 0.05 eV at a coverage of 4.3 ML) is different from that observed for the Si face due to a different surface band bending, which is a result of the face-specific Schottky barrier height between SiC and FLG.[40] The second component is due to the growing FLG layer. Its binding energy is 284.65 ± 0.05 eV for the lowest coverage (0.15 ML) and 284.42 ± 0.05 eV for the highest coverage (4.3 ML), which is characteristic of graphite. The slightly higher binding energy at low coverage is again attributed to *n*-type doping by the substrate. Other than that, the bonding in the overlayer is—from the beginning—practically identical with that in graphene, i.e., strong sp^2 bonding within the graphene

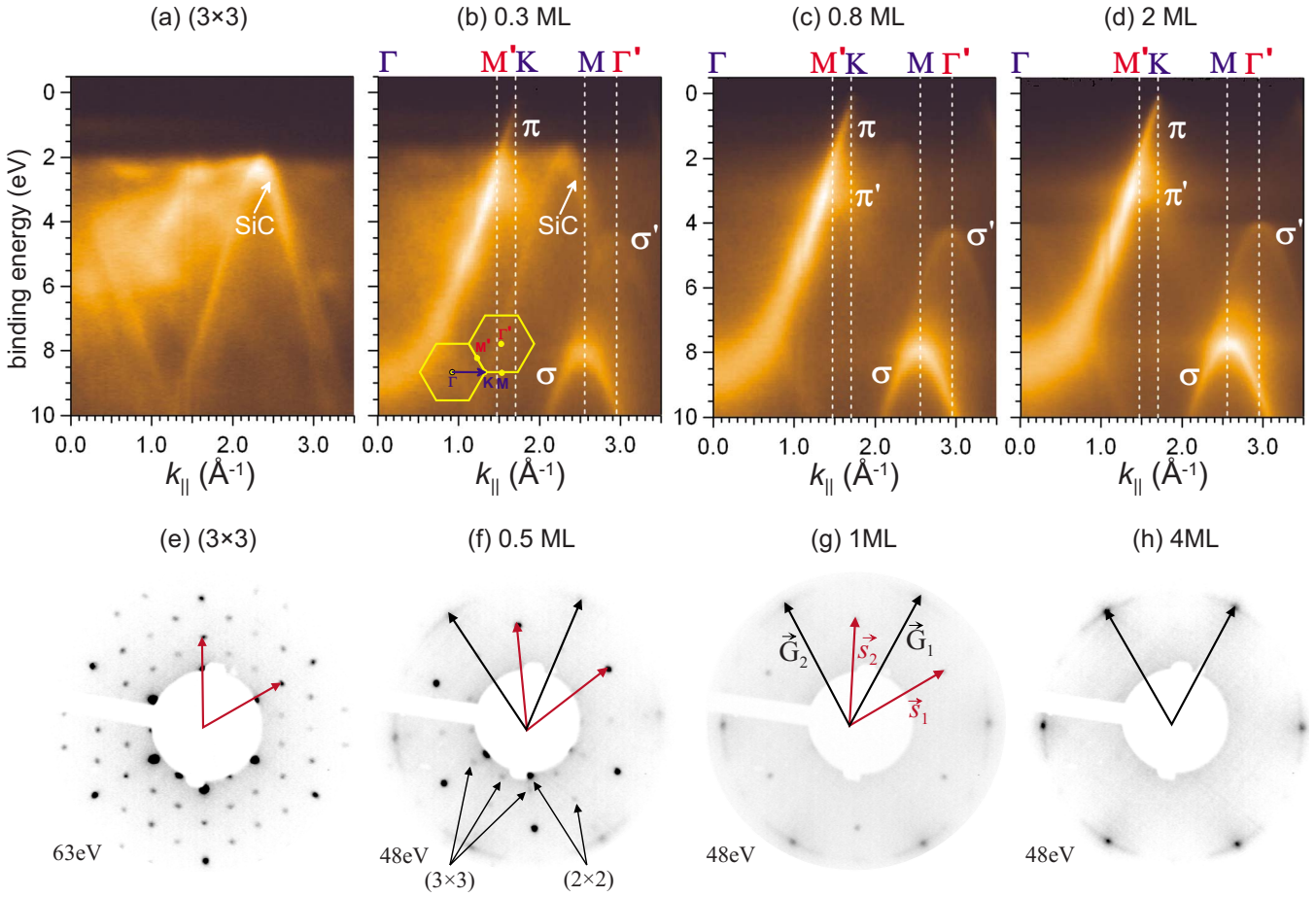

FIG. 4. (Color online) [(a)–(d)] Photoelectron intensity map vs binding energy and parallel electron momentum acquired at different stages of FLG growth on SiC(000$\bar{1}$) starting from the clean (3×3) reconstruction. The graphene overlayer thickness determined from the C 1*s* core levels is indicated. The inset in (b) shows the Brillouin zone of graphene with the nominal azimuth marked by the arrow. σ and π mark the σ and π bands, respectively, for the nominal azimuth. σ' and π' indicate the σ and π bands of rotated domains, respectively. SiC in (a) and (b) marks a prominent SiC bulk band. Photon energy was $h\nu$=65 eV. [(e)–(h)] LEED patterns obtained for various stages of FLG growth. The reciprocal lattice vectors of the SiC $(\vec{s}_1,\vec{s}_2)$ and graphene $(\vec{G}_1,\vec{G}_2)$ lattices are indicated.

layers and weak interaction among the layers and with the substrate.

IV. DISCUSSION

A. Interface between few layer graphene and SiC(0001)

Our experimental results provide strong evidence that the $6\sqrt{3}$ reconstruction formed on the (0001) surface of SiC during the initial stage of graphitization comprises a single layer of C atoms with graphene-like atomic arrangement, which interacts with the underlying surface by covalent bonds so that its electronic structure deviates from that of graphene in the region of the π bands. Hence, a weak bonding by van der Waals interaction to either the SiC(0001)-(1×1) surface, as proposed in Refs. 9 and 41, or to the Si-rich $(\sqrt{3}\times\sqrt{3})R30°$ reconstruction, as in Refs. 11, 42, and 43, can be ruled out. The strong coupling of that layer to the substrate surface is in agreement with the theoretical CSG model.[19–21] Due to the covalent bonding, the graphene π states retreat from E_F and open a gap in the electronic structure of the $6\sqrt{3}$ reconstruction. The reconstruction layer[53] is present at the interface between the SiC(0001) substrate and the growing FLG stack. Graphene layers beyond the interface layer have true graphene properties.

This is, however, as far as the agreement with the calculations of Refs. 19–21 go. For the $6\sqrt{3}$ reconstruction, we find two surface states (g_1 and g_2) that are located below E_F but are not present in the calculations. Further, contrary to experiment that clearly shows a semiconducting surface, the calculations[19–21] have a half-filled band that renders the model surface metallic. This band arises from unsaturated Si dangling bonds [one per artificial $(\sqrt{3}\times\sqrt{3})R30°$ unit cell as seen in Fig. 1] that form a half-filled and, thus, metallic band.

Two explanations for this failure to describe the real situation come to mind. First, strong correlations within the Si dangling bond band could lead to a Mott–Hubbard (MH) metal-insulator transition. Such MH transitions appear to be the rule rather than the exception on SiC surfaces (see, for example, Refs. 44 and 45 and references therein). However, this possibility was excluded by the authors of Refs. 20 and 21.

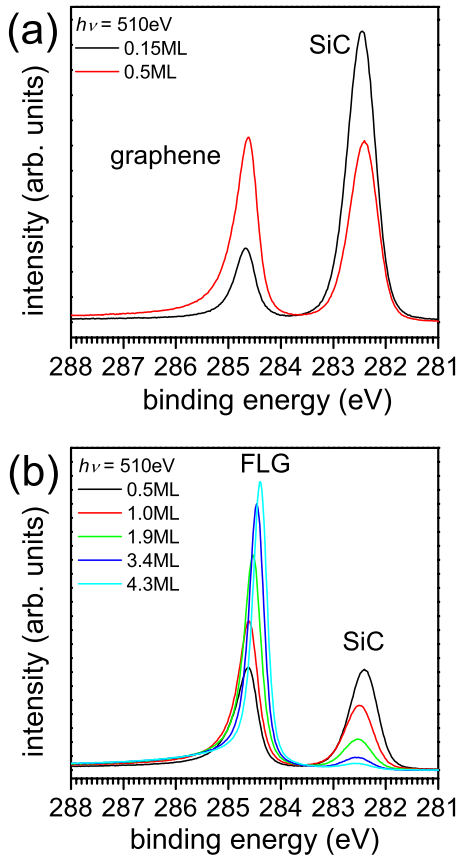

FIG. 5. (Color online) (a) CIS core-level spectra of the initial stage of graphene formation on the SiC(000$\bar{1}$) surface with a coverage of 0.15 and 0.5 ML. (b) C 1*s* core-level spectra after subsequent growth of up to 4.3 layers of graphene on the C face.

On the other hand, the question remains if the predicted metallicity of the interface, which is not experimentally observed, is a consequence of the artificially chosen $(\sqrt{3}\times\sqrt{3})R30°$ unit cell in the calculations vs the much larger $6\sqrt{3}$ unit cell experimentally observed in LEED. An independent experimental estimate of the number of Si dangling bonds is provided by the S1/S2 ratio of 0.50 ± 0.08 [see Fig. 3(a)], which implies that $33\pm4\%$ of the C atoms in the $6\sqrt{3}$ reconstruction layer are bonded to underlying Si atoms of the substrate. The $6\sqrt{3}$ unit mesh on the SiC(0001) surface, which covers 108 Si atoms of the topmost SiC bilayer, corresponds to a (13×13) supercell of graphene that includes 338 C atoms. Hence, the ratio of Si in the topmost SiC bilayer to C atoms in the covalently bound reconstruction layer is 0.32, which compares surprisingly well with the value of 0.33 ± 0.04 obtained from the S1/S2 ratio. This suggests that nominally all Si atoms in the SiC(0001) surface form Si-C bonds to the reconstruction layer. The experimental error allows for a maximum of around ten Si dangling bonds per $6\sqrt{3}$ unit cell, which is less than one-third of the number of dangling bonds assumed by the CSG model. The SiC(0001) surface lattice and the graphene lattice are incommensurate, i.e., when graphene is placed on top of the SiC(0001) surface, not every Si atom has a C atom directly above it (see Fig. 1). However, as was shown in previous work, the Si atoms on the SiC(0001) surface show considerable flexibility in both bond angle and bond length.[46–48] The misfit between the graphene and SiC surface lattices could thus be accommodated by small variations of bond angles and distances, leaving behind only a small number of dangling bonds at defect sites. In agreement with that, there is evidence of disorder within the $6\sqrt{3}$ unit cell as witnessed by a spatially inhomogeneous tunneling probability in STM micrographs.[33,38,41,49] A disordered array of low concentration Si dangling bonds is certainly detrimental for the formation of a Si dangling bond derived band. Instead, one expects localized states where the considerable correlation energy separates empty and singly occupied states from the double occupied ones by the correlation energy.

B. Interface between few layer graphene and SiC(000$\bar{1}$)

By comparing our experimental results for the graphene/SiC(000$\bar{1}$) interface with the CSG model,[19–21] we note several differences. Our ARPES data undoubtedly prove that already at the monolayer coverage the graphene-like band dispersion of the overlayer is fully developed. Also, the C1*s* spectra show the dominant surface component associated with graphene without any indication of covalent bonding to the substrate. Finally, LEED and ARPES data clearly show that from the very beginning of growth, the graphene layers on SiC(000$\bar{1}$) exist in rotated domains, which is a consequence of the weak interaction with the substrate. In contrast, the CSG model assumes a strong covalent bond between SiC(000$\bar{1}$) and the first graphene layer, such that the latter lacks a graphene-like π band and is thereby locked in its orientation to the substrate. Only when the second layer is added do the calculations yield a graphene band structure. Hence, based on our experimental data, we can exclude the CSG model in all aspects as representative of the graphene/SiC(000$\bar{1}$) interface.

Why do the two surface polarities behave so different? Naively, one could expect that the $6\sqrt{3}$ reconstruction is observed on both Si and C faces. However, based on the results obtained by density functional theory calculations,[46,50] it becomes clear that the two surface polarities are quite different. Compared to the Si face, the C face shows a considerably stronger inward relaxation of the outermost C atoms accompanied by a three times larger relaxation energy, which makes changes in bond lengths and angles harder as compared to the Si face. Second, whereas the charge density of the Si dangling bond on the Si face is predominantly directed away from the surface, the charge density of the much smaller C dangling bond has its maximum mostly within the surface plane. ARPES measurements of the surface electronic structure of unreconstructed SiC{0001} surfaces have revealed that the dispersion of the C dangling bond band is unexpectedly large, indicating a larger degree of delocalization, which was attributed to hybridization with bulk states.[45] Based on these findings, a covalent bond between the C atoms on SiC(000$\bar{1}$) and an overlying graphene layer in a fashion similar to what we have proposed above for the (0001) surface appears much less likely. This could explain the dif-

ference in bonding between the polar SiC{0001} surfaces and graphene observed here.

Based on x-ray reflectivity data, Hass *et al.*[51] recently suggested a model with a carbon rich interface layer. This model is expected to lead to a chemically shifted interface component in the C1*s* spectra with an intensity similar to that of the surface components S1/S2 observed for the $6\sqrt{3}$ reconstruction on the Si face [see Fig. 3(a)]. Also, one would expect additional states in the valence band spectra, which are not observed here. This indicates that the model does not apply. Furthermore, the x-ray reflectivity study finds a short bond length between the SiC substrate and the first graphene layer, which was interpreted as a strong chemical bond to the surface in agreement with the calculations.[19–21] According to the ARPES and SXPS data presented above, there is not the slightest indication of a covalent bond of the first graphene layer to the SiC$(000\bar{1})$ surface. We cannot provide a final explanation for the disagreement between our study and the x-ray reflectivity study.[51] However, we note that the interpretation of x-ray reflectivity data requires fitting interface models with many adjustable parameters such as layer distances and layer dependent atomic densities. On the other hand, our ARPES and SXPS results reflect the electronic and chemical properties of the surface in a much more direct way and, most importantly, without modeling.

C. Bonding and ordering of few layer graphene

The differences in interfacial bonding between the bottom carbon layer and the two SiC{0001} surfaces of different polarities play a decisive role in determining the structural properties of graphene films on these surfaces. As discussed above, the interaction of FLG with the underlying substrate differs with surface polarity. For FLG on the SiC(0001) surface, we observe a strong covalent interaction of the $6\sqrt{3}$ reconstruction layer with the substrate, which persists at the interface between SiC(0001) and thicker FLG films. This strong bond is responsible for the orientation of the reconstruction layer, which shows a rotation angle of 30° with respect to the substrate and gives rise to the $6\sqrt{3}$ reconstruction. We also see that the $6\sqrt{3}$ reconstruction remains present at the interface upon further graphitization. ARPES experiments[26–28,34] indicate that the first and the following graphene layers on top of the interface layer have a true graphene or FLG electronic structure and, therefore, interact only weakly by van der Waals forces with the $6\sqrt{3}$ interface layer. Nevertheless, they maintain the rotational order relative to the substrate imprinted by the $6\sqrt{3}$ interface layer. On the other hand, for FLG on SiC$(000\bar{1})$, a weak interaction allows for a different orientation of the nucleating graphene layers relative to the substrate. Furthermore, it was observed that FLG films on SiC$(000\bar{1})$ contain rotational stacking faults, i.e., that the individual graphene layers do not follow the Bernal *AB* ordering[17,51] typical for graphite. Weak interactions between subsequent graphene layers apparently allow for rotational stacking faults that are energetically not too different from the *AB* stacking of graphite[52] and, hence, leads to the turbostratic structure of FLG on SiC$(000\bar{1})$.

If the FLG films would grow in a layer-by-layer mode such that new graphene layers are formed on top of already existing ones, including the $6\sqrt{3}$ reconstruction layer, one would expect that a rotational disorder is observed for the Si-terminated (0001) surface as well, which is at odds with the observations listed above. Hence, we suggest that the FLG films grow by forming new graphene layers right at the interface. This is, indeed, reasonable since the source of the growing film is the substrate itself. At the growth temperatures in excess of 1150 °C, Si-C bonds are statistically broken. While it is not possible to form stable, i.e., long lasting, Si-Si bonds at this temperature, C-C bonds are stable. Thus, the Si atoms will diffuse away and eventually sublimate from the surface, whereas the carbon atoms will nucleate into graphene.

On the Si face, the nucleation of a new layer takes place *underneath* the reconstruction layer. Consider that, due to the high temperature, a Si atom of the topmost SiC bilayer leaves its position and a Si vacancy is created. This leaves behind three C atoms of the top SiC bilayer, each of them carrying a dangling bond that is directed roughly towards the other two. At the same time, an unsaturated orbital is created on the C atom in the reconstruction layer that was previously bound to Si. That C atom cannot bind to one of the C dangling bonds left behind in the SiC substrate because they are too far away and point in the wrong direction. Instead, the unsaturated C atom of the reconstruction layer can easily rehybridize and form an additional π bond with the neighboring C atoms in the reconstruction layer. No rearrangement of carbon atoms is necessary for this process, but only a cutting of C-Si bonds. Eventually, all bonds of the reconstruction layer to the SiC surface are broken and this layer becomes the first graphene layer proper. The unsaturated C atoms created in the topmost SiC bilayer will not be satisfied with the situation. Instead, they can form stable C-C bonds with each other and nucleate into graphene, which is covalently bound to the substrate as described above. Thus, the newly nucleating graphene layer takes on the role of the interface layer with its fixed azimuthal relationship to the substrate. In this way each graphene layer starts out as a $6\sqrt{3}$ layer with an orientation that is dictated by the covalent bonds to the substrate. Hence, there is no freedom for the growing FLG layer to form rotated domains and *rotational* stacking faults. On the other hand, we have to note that the covalent bonds between the interface layers and the SiC(0001) surface determine the lateral registry between the individual graphene layers after they have been released. This undoubtedly will lead to *linear* stacking faults in the growing graphite stack. Indeed, an evidence for the presence of such linear stacking faults in epitaxial graphene layers[7] (up to 4 ML thick) has been observed by ARPES[27] and STM.[39]

On the C face, the situation is different. As discussed above, there is a weak interaction between the bottom graphene layer and the SiC$(000\bar{1})$ surface. Consider the formation of a Si vacancy at the interface. This results in three C atoms, each of them carrying two dangling bonds, one of them pointing into the vacancy and one pointing away from the surface. The only possibility for the C atoms to saturate

their dangling bonds is by forming C-C bonds as there are no unsaturated Si atoms nearby. This marks the nucleation of a new graphene layer. Removing all Si atoms from the surface bilayer leaves a C-terminated surface to which the nucleating graphene apparently does not bind covalently. As a result, the graphene nuclei experience weak constraints, such that they orient with different rotation angles with respect to the substrate and the other graphene layers.[17] This leads to the turbostratic nature of the graphitic films on the C face observed by x-ray diffraction[17] and STM.[18]

V. CONCLUSIONS

We have investigated few layer graphene films (FLG) thermally grown on the two polar SiC surfaces by angle-resolved photoelectron spectroscopy, high-resolution core-level photoelectron spectroscopy, and low-energy electron diffraction with special emphasis on the properties of the interface between graphene and the SiC substrate. From our experiments and the discussion presented above, the following conclusions can be drawn.

On the Si-terminated (0001) surface, the $6\sqrt{3}$ reconstruction represents a structure *sui generis* that provides the interface between SiC and all following graphene layers. It consists of a carbon layer with graphene-like topology and bond length as witnessed by σ bands that are identical to those of graphene. Every third carbon atom, however, is covalently bonded to the underlying Si atoms that terminate the bulk 6*H*-SiC. As such, there is no room for a half-filled dangling-bond-derived band that would account for the metallic nature of the interface as proposed in Refs. 19–21 Instead, the $6\sqrt{3}$ surface is semiconducting, with Si dangling bonds present at best as localized defect states at the interface.

The $6\sqrt{3}$ structure remains unaltered at the interface during subsequent growth. The first, second, and further graphene layers weakly interact with the $6\sqrt{3}$ interface layer and exhibit the electronic structure of graphene and graphene stacks in accordance with earlier studies.

On the C-terminated SiC$(000\bar{1})$ surface, all our data indicate only a weak interaction of graphene with the substrate and no distinct interface phase. From the beginning, carbon atoms thermally released from the SiC substrate nucleate into sp^2-hybridized islands such that the band structure characteristic of graphene is fully developed already at the monolayer coverage albeit with clear signs of azimuthal disorder.

Azimuthal disorder beyond the first graphene layer is expected for both surfaces on account of the high growth temperature and the weak interlayer interaction; it is known in the field of graphite as turbostratic growth. Hence, it comes as little surprise for FLG on SiC$(000\bar{1})$. In the light of that, the high degree of azimuthal ordering in FLG on SiC(0001) even beyond the first graphene layer is rather surprising. It can be explained by a different growth model that we propose here. Each new graphene layer is formed at the bottom of the FLG stack by releasing the graphene-like carbon of the $6\sqrt{3}$ interface from the substrate as Si atoms evaporate, while a new $6\sqrt{3}$ interface layer is formed. In this way, the azimuthal orientation of the interface layer is inherited by each new graphene layer, while linear stacking faults are possible.

ACKNOWLEDGMENTS

We thank E. Rotenberg, K. Horn, T. Ohta, A. Bostwick, J. L. McChesney, and L. Hammer for fruitful and stimulating discussions, and the staff of BESSY, especially W. Braun, G. Gavrila, A. Varykhalov, and M. Sperling for their continuing support. Travel to BESSY was funded by the BMBF under Contract No. 05 ES3XBA/5.

*Corresponding author; thomas.seyller@physik.uni-erlangen.de; URL: http://www.tp2.uni-erlangen.de

[1] C. Berger *et al.*, J. Phys. Chem. B **108**, 19912 (2004).
[2] K. S. Novoselov, A. K. Geim, S. V. Morozov, D. Jiang, Y. Zhang, S. V. Dubonos, I. V. Grigorieva, and A. A. Firsov, Science **306**, 666 (2004).
[3] K. S. Novoselov, A. K. Geim, S. V. Morozov, D. Jiang, M. I. Katsnelson, I. V. Grigorieva, S. V. Dubonos, and A. A. Firsov, Nature (London) **438**, 197 (2005).
[4] Y. Zhang, Y.-W. Tan, H. L. Störmer, and P. Kim, Nature (London) **438**, 201 (2005).
[5] C. Berger *et al.*, Science **312**, 1191 (2006).
[6] K. S. Novoselov, E. McCann, S. V. Morozov, V. I. Falko, M. I. Katsnelson, U. Zeitler, D. Jiang, F. Schedin, and A. Geim, Nat. Phys. **6**, 177 (2006).
[7] K. S. Novoselov, Z. Jiang, Y. Zhang, S. V. Morozov, H. L. Störmer, U. Zeitler, J. C. Maan, G. S. Boebinger, P. Kim, and A. K. Geim, Science **315**, 1379 (2007).
[8] A. K. Geim and K. S. Novolselov, Nat. Mater. **6**, 183 (2007).
[9] A. J. Van Bommel, J. E. Crombeen, and A. Van Tooren, Surf. Sci. **48**, 463 (1975).
[10] L. I. Johansson, F. Owman, and P. Mårtensson, Phys. Rev. B **53**, 13793 (1996).
[11] I. Forbeaux, J. M. Themlin, and J. M. Debever, Phys. Rev. B **58**, 16396 (1998).
[12] L. I. Johansson, P. A. Glans, and N. Hellgren, Surf. Sci. **405**, 288 (1998).
[13] I. Forbeaux, J. M. Themlin, and J. M. Debever, Surf. Sci. **442**, 9 (1999).
[14] U. Starke, M. Franke, J. Bernhardt, J. Schardt, K. Reuter, and K. Heinz, Mater. Sci. Forum **264-268**, 321 (1998).
[15] U. Starke, J. Schardt, and M. Franke, Appl. Phys. A: Mater. Sci. Process. **65**, 587 (1997).
[16] J. Hass, R. Feng, T. Li, X. Li, Z. Zong, W. A. de Heer, P. N. First, E. H. Conrad, C. A. Jeffrey, and C. Berger, Appl. Phys. Lett. **89**, 143106 (2006).
[17] J. Hass, F. Varchon, J. E. Millán-Otoya, M. Sprinkle, N. Sharma, W. A. de Heer, C. Berger, P. N. First, L. Magaud, and E. H. Conrad, Phys. Rev. Lett. **100**, 125504 (2008).
[18] M. Naitoh, M. Kitada, S. Nishigaki, N. Toyama, and F. Shoji,

Surf. Rev. Lett. **10**, 473 (2003).
[19] F. Varchon *et al.*, Phys. Rev. Lett. **99**, 126805 (2007).
[20] A. Mattausch and O. Pankratov, Phys. Rev. Lett. **99**, 076802 (2007).
[21] A. Mattausch and O. Pankratov, Mater. Sci. Forum **556-557**, 693 (2007).
[22] T. Seyller *et al.*, Surf. Sci. **600**, 3906 (2006).
[23] U. Starke, in *Recent Major Advances in SiC*, edited by W. Choyke, H. Matsunami, and G. Pensl (Springer Scientific, New York, 2003), p. 281.
[24] L. Broekman, A. Tadich, E. Huwald, J. D. Riley, R. C. G. Leckey, T. Seyller, K. V. Emtsev, and L. Ley, J. Electron Spectrosc. Relat. Phenom. **144**, 1001 (2005).
[25] J. D. Joannopoulos and M. L. Cohen, Phys. Rev. B **7**, 2644 (1973).
[26] A. Bostwick, T. Ohta, T. Seyller, K. Horn, and E. Rotenberg, Nat. Phys. **3**, 36 (2007).
[27] T. Ohta, A. Bostwick, J. L. McChesney, T. Seyller, K. Horn, and E. Rotenberg, Phys. Rev. Lett. **98**, 206802 (2007).
[28] T. Ohta, A. Bostwick, T. Seyller, K. Horn, and E. Rotenberg, Science **313**, 951 (2006).
[29] J. Voit, L. Perfetti, F. Zwick, H. Berger, G. Margaritondo, G. Grüner, H. Höchst, and M. Grioni, Science **290**, 501 (2000).
[30] A. Nagashima, N. Tejima, and C. Oshima, Phys. Rev. B **50**, 17487 (1994).
[31] J. O. Sofo, A. S. Chaudhari, and G. D. Barber, Phys. Rev. B **75**, 153401 (2007).
[32] E. J. Duplock, M. Scheffler, and P. J. D. Lindan, Phys. Rev. Lett. **92**, 225502 (2004).
[33] W. Chen, H. Xu, L. Liu, X. Gao, D. Qi, G. Peng, S. C. T. Y. Feng, K. P. Loh, and A. T. S. Wee, Surf. Sci. **596**, 176 (2005).
[34] A. Bostwick, T. Ohta, J. L. McChesney, K. V. Emtsev, T. Seyller, K. Horn, and E. Rotenberg, New J. Phys. **9**, 385 (2007).
[35] P. Mallet, F. Varchon, C. Naud, L. Magaud, C. Berger, and J.-Y. Veuillen, Phys. Rev. B **76**, 041403(R) (2007).
[36] G. M. Rutter, J. N. Crain, N. P. Guisinger, T. Li, P. N. First, and J. A. Stroscio, Science **317**, 219 (2007).
[37] V. W. Brar, Y. Zhang, Y. Yayon, T. Ohta, J. L. McChesney, A. Bostwick, E. Rotenberg, K. Horn, and M. F. Crommie, Appl. Phys. Lett. **91**, 122102 (pages 3) (2007).
[38] C. Riedl, U. Starke, J. Bernhardt, M. Franke, and K. Heinz, Phys. Rev. B **76**, 245406 (2007).
[39] P. Lauffer, K. V. Emtsev, R. Graupner, T. Seyller, L. Ley, S. A. Reshanov, and H. B. Weber, Phys Rev. B (to be published).
[40] T. Seyller, K. Emtsev, F. Speck, K.-Y. Gao, and L. Ley, Mater. Sci. Forum **556-557**, 701 (2007).
[41] M. H. Tsai, C. S. Chang, J. D. Dow, and I. S. T. Tsong, Phys. Rev. B **45**, 1327 (1992).
[42] J. E. Northrup and J. Neugebauer, Phys. Rev. B **52**, R17001 (1995).
[43] V. Van Elsbergen, T. Kampen, and W. Mönch, Surf. Sci. **365**, 443 (1996).
[44] F. Bechstedt and J. Furthmüller, J. Phys.: Condens. Matter **16**, S1721 (2004).
[45] K. V. Emtsev, T. Seyller, L. Ley, L. Broekman,A. Tadich, J. D. Riley, R. G. C. Leckey, and M. Preuss, Phys. Rev. B **73**, 075412 (2006).
[46] M. Sabisch, P. Krüger, and J. Pollmann, Phys. Rev. B **55**, 10561 (1997).
[47] U. Starke, J. Schardt, J. Bernhardt, M. Franke, K. Reuter, H. Wedler, K. Heinz, J. Furthmüller, P. Käckell, and F. Bechstedt, Phys. Rev. Lett. **80**, 758 (1998).
[48] U. Starke, J. Schardt, J. Bernhardt, M. Franke, and K. Heinz, Phys. Rev. Lett. **82**, 2107 (1999).
[49] F. Owman and P. Mårtensson, Surf. Sci. **369**, 126 (1996).
[50] A. Mattausch, T. Dannecker, and O. Pankratov, Mater. Sci. Forum **556-557**, 493 (2007).
[51] J. Hass, R. Feng, J. E. Millan-Otoya, X. Li, M. Sprinkle, P. N. First, W. A. de Heer, E. H. Conrad, and C. Berger, Phys. Rev. B **75**, 214109 (2007).
[52] A. N. Kolmogorov and V. H. Crespi, Phys. Rev. B **71**, 235415 (2005).
[53] For the covalently bound graphene layer, we will use the two terms *reconstruction layer* and *interface layer* depending on whether we discuss the bare $6\sqrt{3}$ reconstruction or the interface between SiC(0001) and FLG, respectively.